

# Estimating Remaining Fatigue Life of Critical Members of Steel Railway Bridges using Fatigue Crack Growth Model

V. Viththagan, R.J. Wimalasiri and P.A.K. Karunananda

**Abstract:** Fatigue failure of steel structures is one of the most urgent study areas due to the inherent catastrophic nature of the failure. Engineers have made a substantial contribution to the understanding of the fatigue phenomenon through several approaches. Heavy cyclic loads imposed on steel railway bridges have the potential to cause cracks in structurally important members. Initiated cracks propagate during its service and lead to a complete structural failure. Since it is not practical to continuously monitor the structural health of bridges, an accurate life prediction approach is necessary to predict failure. This study proposes the fracture mechanics approach for fatigue life prediction of the critical members of bridges. Standard compact tension C(T) specimens were prepared with a pre-crack to test the fatigue crack growth rate under different stress levels. The crack growth rate  $da/dN$  was calculated by plotting the crack length ( $a$ ) vs the number of cycles ( $N$ ). According to ASTM E647-15, the stress intensity factor range ( $\Delta K$ ) for the C(T) specimen was determined. Under the conditions of constant amplitude loading, a modified version of the Paris law was used to construct an empirical relationship between  $da/dN$  and  $\Delta K$ . The results of the vibration analysis were used to validate the finite element model of a case study railway bridge in Sri Lanka. The Finite Element (FE) method was used to assess the life of the most critical bridge member, and its estimated remaining fatigue life is 14.5 years.

**Keywords:** Fracture mechanics, Fatigue failure, Steel bridge, Crack propagation

## 1. Introduction

The fatigue of materials can be traced back to the first half of the 19th century. Since then engineers and researchers have made contributions to understanding the phenomenon called fatigue. Fatigue failure is critical since it initiates cracks microscopically at low-stress levels than to the allowable stress when the structure is subjected to cyclic loading. Numerous studies have been conducted recently on the impact of various microstructural, mechanical, and environmental parameters on fracture initiation and growth, cyclic deformation, and other engineering-related phenomena in a variety of materials [1].


When it comes to Sri Lankan railway bridges, metal bridges were introduced in the 19th century, and most of the bridges are still in operation even after a century [2]. Sri Lankan railways started using heavy engines to operate at their maximum speed and efficiency which generate heavy cyclic loads on the bridges.

Most of the structural members of the bridge have started to deform, and some of them have

even developed fractures due to cyclic loads [2, 3].

Railway bridges in Sri Lanka are regularly experiencing high cyclic loads which cause cracks and eventually lead to a total structural failure. Since it is not always possible to monitor bridges continuously, an accurate life prediction approach is needed to identify failure and reduce significant accidents. Stress-life and fracture mechanics approaches are currently adopted to study and analyze the life of steel bridges [4,5].


**Eng. V. Viththagan**, AMIE(SL), B.Tech (Eng) (NIT), AEng(ECSL), Workshop Engineer at the Department of Mechanical Engineering, The Open University of Sri Lanka. Email: [vvith@ou.ac.lk](mailto:vvith@ou.ac.lk)

 <https://orcid.org/0000-0003-0615-9066>

**Dr. R.J. Wimalasiri**, BTech (Eng) (Hons) (OUSL), PhD (SHU), Senior Lecturer at the Department of Mechanical Engineering, The Open University of Sri Lanka. Email: [rjwim@ou.ac.lk](mailto:rjwim@ou.ac.lk)

 <https://orcid.org/0000-0001-8368-5639>

**Eng. (Dr.) P.A.K. Karunananda**, B. Eng., MIE(Sri Lanka), B.Sc. Eng. (Peradeniya), M. Phil. (Peradeniya), MEng. (Ehime), D.Eng. (Ehime), Senior Lecturer, Department of Civil Engineering, Open University of Sri Lanka. Email: [pakar@ou.ac.lk](mailto:pakar@ou.ac.lk)

 <https://orcid.org/0000-0001-9581-7440>

The crack initiation and propagation aspects may be thoroughly examined using the fracture mechanics approach, which is suitable for lifetime estimations and failure predictions of bridges. A technique is required to predict the lifetime of the bridge or, more particularly, the critical members of the bridge, as the failure of railway bridges is catastrophic. The results would lead to identifying fatigue performance of bridges, formulating a well-planned inspection routine, and strengthening and repair schedules, which could ensure continuous and satisfactory performance of bridges during their service life.

In this study, a railway bridge in a coastal railway line was visually inspected and deformation and cracks were identified. A crack was identified in one of the connecting plates shown in Figure 1 and it is being replaced periodically during the routine maintenance by the Sri Lanka Railway Department.

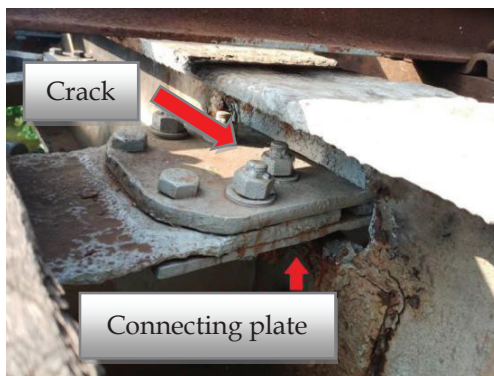


**Figure 1 - Connecting Plate in the Bridge**

This paper aims to determine the crack propagation rate of the material under different loading conditions, formulate the theoretical framework crack growth rate based on the fracture mechanics approach and predict the fatigue life of the critical member of the bridge.

## 2. Methodology

The methodology followed in this study is summarized as follows.

### 2.1. Vibration Analysis

The live load history of the selected bridge members was obtained by performing a vibration analysis. A triaxial accelerometer was placed on the selected members while the class M4 locomotive is crossing the bridge at the given time. M4 is the class of locomotive which has a 98-ton loco weight. High stresses experienced by the bridge member during the

testing were determined using the velocity vs frequency spectrum (Figure 2) and the empirical relationship in (Equation 1) [6,7].

$$\sigma_{max} = V_{max} \frac{h}{\eta} \sqrt{E\rho} \quad \dots (1)$$

where,  $\sigma_{max}$  is the maximum modal stress,  $V_{max}$  is the maximum modal velocity,  $E$  is Young's modulus,  $\rho$  is density,  $h$  is the cross-sectional distance from neutral axis and  $\eta$  is radius gyration.

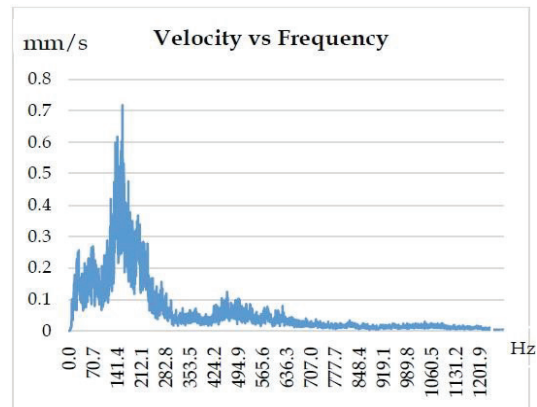


**Figure 2 - Vibration Spectrum of the Connecting Plate**

The steel bridge was modelled using the software SOLIDWORKS and numerically analysed to determine the stresses acting on the connecting plate at different loading combinations. Stresses on the connecting plate were determined when the train is at different locations (12 distances from the initial point) inside the bridge [7]. Figure 3 shows the maximum and minimum stresses on the bridge among the loading combinations.

Results obtained from the vibration analysis (using Equation 1) and the finite element (FE) model were compared (Figure 4). FE results show a good agreement with the experimental results and the numerical model has been validated [7].

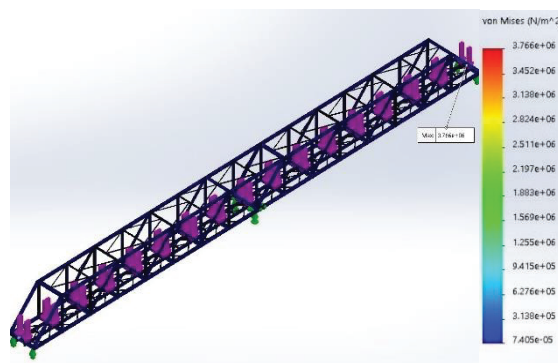


**Figure 3(a)**

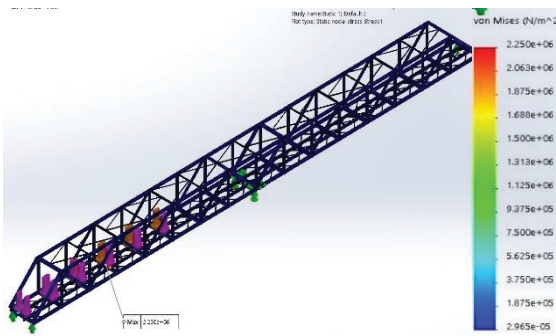


Figure 3(b)

Figure 3 - (a) Maximum, 3 (b) Minimum Stress on the Bridge

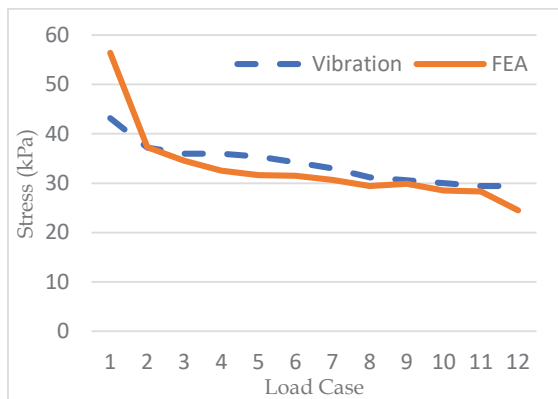


Figure 4 - Comparison of Vibration and FE Results

## 2.2. Material Properties

Steel samples were collected from the railway bridge during routine maintenance. Tensile testing specimens were prepared and tested following the ASTM E8/E8M-09 Standard using the INSTRON 8800 (100 kN load capacity) material testing machine, and generated stress versus strain curve of the material is shown in Figure 5.

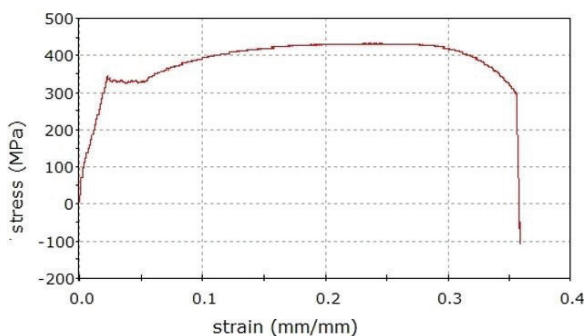


Figure 5 - Stress vs Strain Curve of the Material

The average hardness of the material is HRB 87.7, determined using the digital Rockwell hardness tester following ASTM E18-15 standards. Steel specimens were prepared following ASTM E3-01 to investigate the microstructure of the material and it was

obtained using the metallurgical microscope. The average grain size  $25\text{ }\mu\text{m}$  was determined using the mean linear intercept (MLI) method following ASTM E112-10 [7].

Table 1 shows the mechanical properties of the steel used for the construction of the bridge.

Table 1 - Mechanical Properties

Mechanical Properties	Value
Yield strength (MPa)	355
Ultimate tensile strength (MPa)	433
Strain at break (mm/mm)	0.36
Tensile stress at break (MPa)	287

## 2.3 Fatigue Crack Propagation Rate

C(T) specimens were prepared to determine the crack propagation rate of the material following ASTM E647-15 standards. The test was conducted under fully reversed cyclic loading (Stress ratio  $R = -1$ ). Figure 6 shows the experimental setup for determining the crack propagation rate.

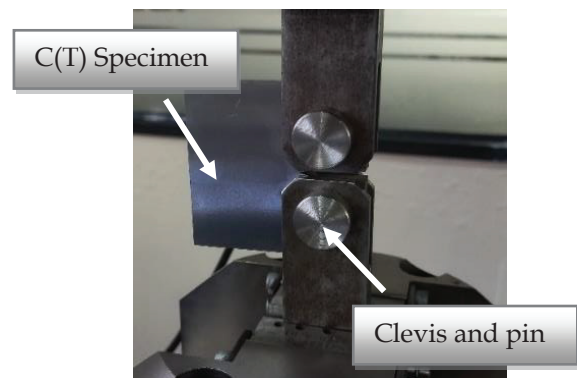


Figure 6 - Specimen Mounted on Instron Machine

Specimens were pre-cracked by applying 2000 cycles under a 12 kN load at 10 Hz. The specimens were tested at different load levels and the crack length was measured using the metallurgical microscope. Figure 7 shows the microscopic view of pre-crack initiated after applying a specific number of cycles.

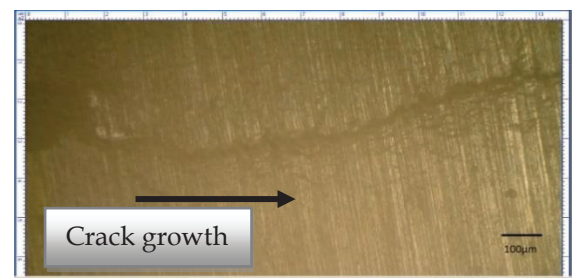


Figure 7 - Microscopic View of Pre-Crack



The crack length was measured every time after a specific number of constant amplitude load cycles was applied. The crack propagation data obtained after each set of cycles is completed and the crack length ( $a$ ) versus number of cycles ( $N$ ) were calculated based on the crack propagation data obtained. The detailed test methods and data are tabulated in Tables 2, 3 and 4.

**Table 2 - Crack Lengths of Specimen No.1**

Load = 15 kN, Frequency = 10 Hz, Pre-crack length = 1.67 mm	
Number of cycles	Final Crack length (mm)
3000	5.45
6000	8.23
9000	11.72
12000	17.80
14000	24.33

**Table 3 - Crack Lengths of Specimen No.2**

Load = 12 kN, Frequency = 10 Hz, Pre-crack length = 1.76 mm	
Number of cycles	Final Crack length (mm)
3000	3.28
6000	4.05
9000	5.21
12000	5.72

**Table 4 - Crack Length of Specimen No.3**

Load = 9 kN, Frequency = 10 Hz, Pre-crack length = 1.36 mm	
Number of cycles	Final Crack length (mm)
3000	2.23
6000	2.66
9000	3.28
12000	3.74
15000	4.22
18000	4.84
23000	5.60
33000	8.08

Above results were used to plot the crack propagation (crack length versus number of cycles) curve at different load levels (15 kN, 12 kN and 9 kN) and the comparison of the curves are shown in Figure 8.

The rate of fatigue crack growth is determined from the crack size versus elapsed cycles data ( $a$  versus  $N$ ). Secant method is followed to determine the crack growth rate in accordance with ASTM E647-15.

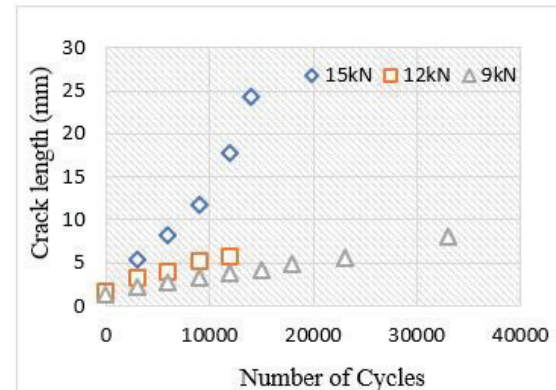


**Figure 8 - Comparison of Crack Propagation Curve at different Load Levels**

The secant or point-to-point technique for computing the crack growth rate simply involves calculating the slope of the straight line connecting two adjacent data points on the ' $a$ ' versus  $N$  curve. It is expressed as follows:

$$\frac{da}{dN} = \frac{(a_{i+1} - a_i)}{(N_{i+1} - N_i)} \quad \dots (2)$$

Crack growth rate of each test (under different loading) can be determined using Equation 2 and the results are shown in Tables 5, 6 and 7.

**Table 5 - Crack Growth Rate of Specimen No.1**

Load = 15 kN, Frequency = 10 Hz, Pre-crack length = 1.67 mm		
Number of cycles	Crack growth (mm)	Crack growth rate ( $da/dN$ )
3000	3.78	0.00126
3000	2.78	0.00093
3000	3.48	0.00116
3000	6.07	0.00203
2000	6.53	0.00327

**Table 6 - Crack Growth Rate of Specimen No.2**

Load = 12 kN, Frequency = 10Hz, Pre-crack length = 1.76 mm		
Number of cycles	Crack length (mm)	Crack growth rate ( $da/dN$ )
3000	1.52	0.00051
3000	0.76	0.00026
3000	1.16	0.00039
3000	0.51	0.00017

**Table 7 - Crack Growth Rate of Specimen No.3**

Load = 9 kN, Frequency = 10 Hz, Pre-crack Length = 1.36 mm		
Number of cycles	Crack length (mm)	Crack growth rate ( $da/dN$ )
3000	0.87	0.00029
3000	0.43	0.00014
3000	0.62	0.00021
3000	0.45	0.00015
3000	0.48	0.00016
3000	0.62	0.00021
5000	0.76	0.00015
10000	2.48	0.00025

#### 2.4 Stress Intensity Factor Range ( $\Delta K$ )

Following ASTM E647-15, for the C(T) specimen, stress intensity factor range ( $\Delta K$ ) can be calculated using following expression.

$$\Delta K = \left( \frac{\Delta P(2+\alpha)}{B\sqrt{W}(1-\alpha)^{1.5}} \right) (0.886 + 4.64\alpha - 13.32\alpha^2 + 14.72\alpha^3 - 5.6\alpha^4) \dots (3)$$

Where  $B$  is thickness,  $W$  is width of the specimen,  $\Delta P$  is force range.

Stress intensity factor range ( $\Delta K$ ) was calculated at the end of each crack propagation and the values are tabulated in Table 8. Figure 9 shows the crack propagation rate ( $da/dN$ ) versus stress intensity factor range ( $\Delta K$ ).

**Table 8 - Calculated Values of Stress Intensity Factor Range**

Load = 15 kN, Frequency = 10 Hz, Pre-crack Length = 1.67 mm			
Number of cycles	Crack growth (mm)	Crack growth rate ( $da/dN$ )	$\Delta K$ (MPa $\sqrt{m}$ )
3000	3.78	0.00126	110.27
3000	2.78	0.00093	127.2
3000	3.48	0.00116	153.05
3000	6.07	0.00203	222.39
2000	6.53	0.00327	385.21

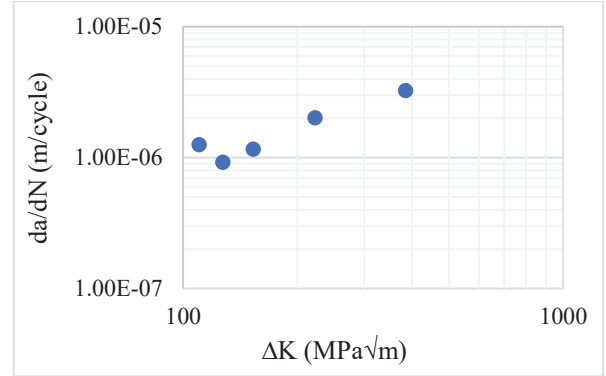


**Figure 9 - Crack Growth Rate Versus Stress Intensity Factor Range Curve**

#### 2.5 Fatigue Crack Growth Model

The crack growth model was developed based on the Paris equation [8] and Equation 3 of the stress intensity factor range for the C(T) specimen. The crack growth rate in the Region II (Figure 10) of the crack growth curve can be explained using linear elastic fracture mechanics and the Paris equation is applicable in this region [9].

$$\frac{da}{dN} = C(\Delta K)^m \dots (4)$$

The relationship between applied load and stress intensity factor range must be determined before any crack growth calculation can be obtained. The most common stress intensity factor form is

$$K = \sigma\sqrt{\pi a} f(a/w) \dots (5)$$

where  $\sigma$  is applied stress,  $a$  is crack length  $f(a/w)$  is geometry term and  $w$  is specimen width. For members such as C (T) specimen, the following expression can be used to determine the stress intensity factor ( $\Delta K_{CT}$ ) (ASTM E647-15).

$$\Delta K_{CT} = \left( \frac{\Delta P(2+\alpha)}{B\sqrt{W}(1-\alpha)^{1.5}} \right) (0.886 + 4.64\alpha - 13.32\alpha^2 + 14.72\alpha^3 - 5.6\alpha^4) \dots (6)$$

where,  $B$  is thickness,  $W$  is width of the specimen and  $\Delta P$  is force range.

Fatigue crack growth rate (Equation 7) can be obtained by combining the Equations 4 and 6.

$$\frac{da}{dN} = C \left[ \left( \frac{\Delta P(2+\alpha)}{B\sqrt{W}(1-\alpha)^{1.5}} \right) (0.886 + 4.64\alpha - 13.32\alpha^2 + 14.72\alpha^3 - 5.6\alpha^4) \right]^m \dots (7)$$

The fatigue life spent during the propagation (Equation 8) can be obtained by integrating Equation 7.

$$N = \int_{a_i}^{a_f} \frac{da}{C \left[ \left( \frac{\Delta P(2+\alpha)}{B\sqrt{W}(1-\alpha)^{1.5}} \right) (0.886 + 4.64\alpha - 13.32\alpha^2 + 14.72\alpha^3 - 5.6\alpha^4) \right]^m} \dots (8)$$

where,  $a_i$  is initial and  $a_f$  is critical crack lengths.

## 2.6 Determination of Parameters

The parameter  $a_i$  is the initial crack size of the test specimen and it is determined by the size of pre-crack. The parameter  $a_f$  is the final crack length of the specimen. Test results of specimen 1 (Table 2) were considered to determine the final crack length after each set of cycles was completed, and the initial and the final crack length values are summarized in Table 9.

**Table 9 - Initial and Final Crack Size after each Set of Cycles**

No. of sets (Cycles)	$a_i$ (mm)	$a_f$ (mm)
Set 1 (3000)	1.67	5.45
Set 2 (6000)	5.45	8.23
Set 3 (9000)	8.23	11.72
Set 4 (12000)	11.72	17.80
Set 5 (14000)	17.80	24.33

The parameters  $B$  and  $W$  represent the thickness and the width of the compact tension C(T) specimen. The value of thickness,  $B = 7\text{mm}$  and width,  $W = 50\text{mm}$ .

$C$  and  $m$  are the material parameters in the mathematical equation, where  $C$  represents the y-axis intercept and  $m$  is slope of the line. The values of  $C$  and  $m$  are determined in experiments and depend on the material, loading ratio, temperature and environmental factors [10]. Figure 10 shows the fatigue crack growth curve approximated by Paris law [11].

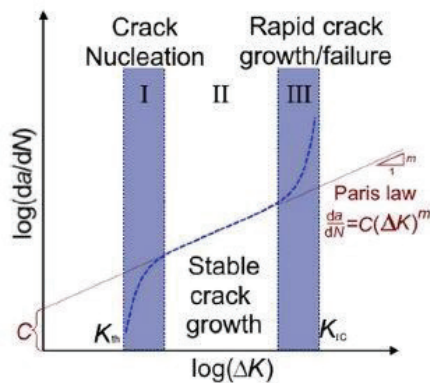


**Figure 10 - Fatigue Crack Growth Curve [11]**

## 2.7. Development of Computer Model

Figure 11 represents the simple chart of the computer model.

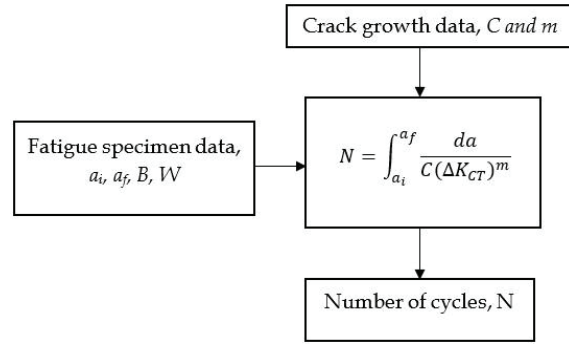


**Figure 11 - Simple Illustration of Mathematical Model**

Microsoft Excel and MATLAB software were used to develop the mathematical model to determine the number of cycles during the propagation. The material constants were determined using the computer model developed by the software.

$$C = 7.36 \times 10^{-9}$$

$$m = 1.203$$

The fatigue crack equation for the specimen becomes as follows,

$$\frac{da}{dN} = 7.36 \times 10^{-9} (\Delta K_{CT})^{1.2} \quad \dots (9)$$

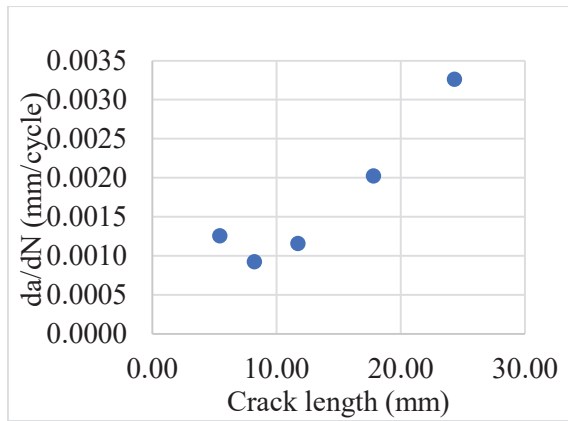
and the number of cycles for crack propagation is given in Equation 10.

$$N = \int_{1.67}^{24.33} \frac{da}{7.36 \times 10^{-9} (\Delta K_{CT})^{1.2}} \quad \dots (10)$$

## 3. Results and Discussions

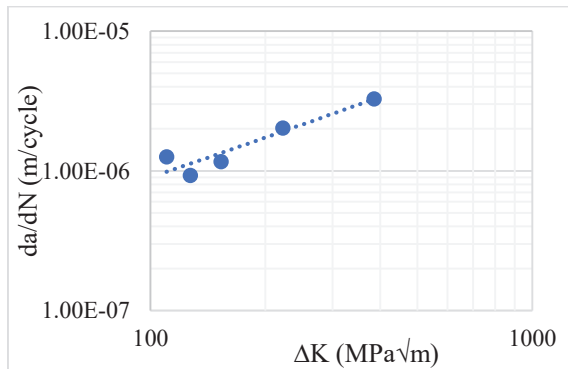
### 3.1 Fatigue Crack Propagation

The crack propagation rate of the specimens was determined under different constant amplitude loading. Figure 8 shows the comparison of the crack propagation curve at loading levels 15 kN, 12 kN, and 9 kN. Even though the crack length increases exponentially with the increasing number of cycles, a reduction of crack propagation can be observed when the crack length reaches 5.45 mm at 15 kN loading (Figure 12). The crack propagation rate under the loads 12 kN and 9 kN are low; also, it can be noted that the crack propagation rate is fluctuating during the crack growth (Table 6, Table 7). The fluctuation occurs due to the crack closure effect during the testing and additional cycles were needed for the crack to grow further.



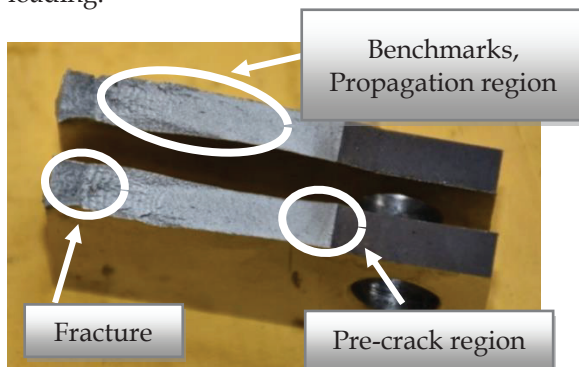
**Figure 12 - Variation of Crack Growth Rate ( $da/dN$ ) against Crack Length ( $a$ ) at 15 kN Loading**

Figure 13 shows the crack propagation curve against the stress intensity factor. According to the curve, it can be assumed that there is a threshold value of stress intensity factor around 110-115  $\text{MPa}\sqrt{\text{m}}$ .



**Figure 13 - Crack Growth Against the Stress Intensity Factor at 15 kN Loading**

Figure 14 shows the surface of the completely failed specimen after 14000 cycles under 15 kN loading.



**Figure 14 - Fracture Surface Regions of C(T) Specimen**

### 3.2 Crack Growth Modelling and Life Time Predictions

The fatigue life determined from the experimental results and the mathematical model were compared. The results are

tabulated in Table 10 with the percentage variation. The initial crack size of the specimen is 1.67 mm and the final crack length ( $a_f$ ) is considered for each set.

**Table 10 - Comparison of Experimental and Mathematical Model**

No. of sets	$a_f$ (mm)	(Exp.) No. of Cycles	(Model) No. of Cycles	Percentage variation %
1	5.45	3000	4574	52.4
2	8.23	6000	6993	16.5
3	11.72	9000	9371	4.1
4	17.80	12000	12391	3.2
5	24.33	14000	14586	4.2

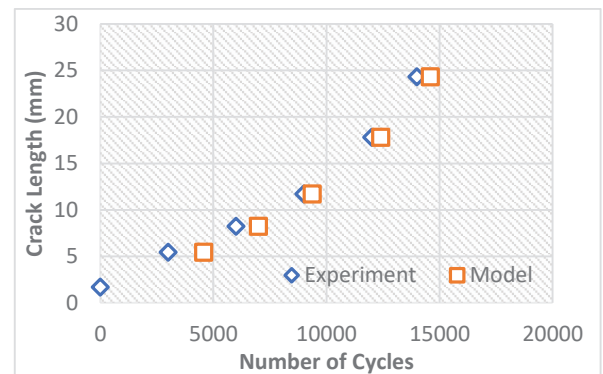


**Figure 15 - Life Time Predictions of Experimental and Mathematical Model**

The comparison shown in Table 13 and Figure 15 suggests the crack propagation results obtained from the experimental and model show a good agreement even though there is a significant variation of 52% when the crack size reaches 5.45 mm. When the crack growth rate against the crack length behaviour is considered (Figure 12), it can be noted that there is a significant reduction in the crack propagation rate when the crack reaches 5.45 mm due to the crack closure. At this point, the mathematical model slightly overpredicts the propagation of the material.

### 3.3 Life Estimation of Critical Members of the Bridge

Identified critical member (connecting plate) was modelled with boundary conditions in finite element analysis software (Ansys 2021 R2) to determine the crack initiation and propagation periods. Figures 16 and 17 show the deformation of the connecting plate when maximum stress was applied and the actual deformed connecting plate which was removed from the railway bridge, respectively.



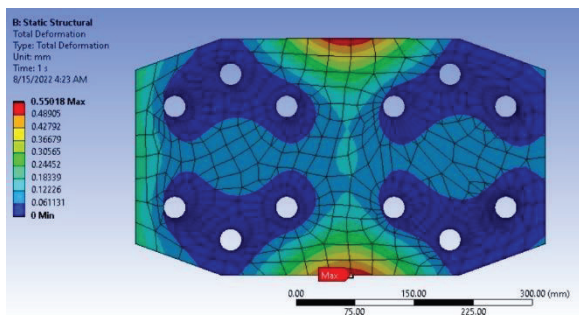


**Figure 16 - FE Analysis of Connecting Plate**



**Figure 17 - Removed Connecting Plate from the Bridge**

From the finite element analysis and the actual deformed connecting plate, it can be noted that the failure of the plate begins at the mid-point of the plate where it experiences maximum stress during loading.

Figure 18 shows the failure analysis of the connecting plate and it can be noted that the connecting plate can withstand nearly 94726 cycles before the crack initiation.

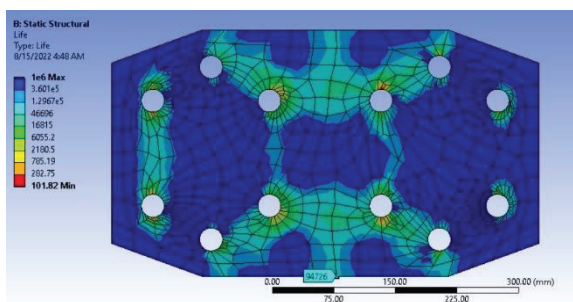


**Figure 18 - Failure Analysis of the Connecting Plate**

The propagation life of the connecting plate can be estimated using the crack propagation model developed with the thickness of the material being 13 mm and the width of the plate being 150 mm. Using MATLAB software, the estimated propagation life of the connecting plate after the crack is initiated is  $5.95 \times 10^5$  cycles and the total life is  $6.89 \times 10^5$  cycles.

Based on the vibration analysis, it was noted that the connecting plate experiences close to maximum velocity six times, each time the train passes the bridge. The number of movements of trains heavier than 98 tons in a day through this particular bridge is 22 [3]. It was assumed that only maximum stress values are influencing the crack propagation therefore number of times the connecting plate experiences the maximum stress in a day is 132. Since it takes  $6.89 \times 10^5$  cycles for the plate to completely fail, the connecting plate can withstand nearly 14.5 years.

## 4. Conclusions

The fatigue performance of high-strength steel has been investigated. Tests to determine the mechanical and material properties were conducted, and the yield strength, ultimate tensile strength, and chemical composition of the material have been determined.

Structural steel S355 has been identified as the material used for the construction of the bridge and the crack propagation rate of the C(T) specimen has been determined experimentally. A crack growth model was developed and material constants related to crack propagation such as  $C$  and  $m$  have been determined.

Using the crack propagation model, the propagation life of the specimen was determined based on the fracture mechanics approach and validated with the experimental results. Mathematical results and experimental results had an initial deviation and that is expected to occur due to the crack propagation reduction due to crack closure and the actual loading conditions.

Identified critical member (connecting plate) was analysed with a finite element model and the initiation and propagation life of the member were determined. A fracture mechanics-based approach to determine the life of the steel railway bridge has been developed and the estimated fatigue life of the critical member is 14.5 years.

## Acknowledgements

The authors wish to acknowledge the Sri Lankan Railway Department for the support given during the testing on the bridge and for providing the material for the lab experiments.



## References

1. Suresh, S. "Fatigue of Materials". 2nd Edition, University of Cambridge, Cambridge, (1998); ISBN 0-521-57847-7.
2. Bandara, C. S., Jayasinghe, J. A. S. C., Karunananda, P. A. K., and Dissanayake, U. I. "Metal used in old Bridges in Sri Lanka and the Effects of their Metal Properties on Capacity Estimations". (2017), *Engineer- Vol.L, No. 03*.
3. Sanjeewa, T.M.K., Madusara, H.A.K.M., Karunarathna, O.G.L.K., and Karunananda, P.A.K., "Fatigue Life Assessment of High Strength Steel Bridges under Corrosion attack: a Sri Lankan Experience". *Department of Civil Engineering, The Open University of Sri Lanka, Nawala, Nugegoda. (2015)*.
4. Chathuranga, D.D.K., Karunanratna, T.E.H., Karannagoda, H.C., Premaratne, R.D.D.N.K., and Karunannanda, P.A.K., "Fatigue Life Estimation of Critical Railway Bridges in KelaniVally Line Sri Lanka". *8th International conference on Structural Engineering and Construction Management, (2017), ICSEM2017-152*.
5. Karunananda, K., Ohga, M., Dissanayake, R., Siriwardane, S., and Chun, P., (2012). "New Combined High and Low Cycle Fatigue Model to Estimate Life of Steel Bridges Considering Interaction of High and Low Amplitude Loadings". *Advances in Structural Engineering. Vol.15. No2*.
6. Gaberson, H. A, "Pseudo Velocity Shock Spectrum Rules for Analysis of Mechanical Shock"; *IMAC XXV, Orlando, FL; Society of Experimental Mechanics; Bethel, CT, www.sem.org; Feb (2007); p 367*.
7. Viththagan, V., Wimalasiri, R.J., and Karunananda, P.A.K., "Condition Assessment of the Critical Members of the Steel Bridges to Improve Reliability". *8th International Symposium on Advances in Civil and Environmental Engineering Practices for Sustainable Development (ACEPS) 2021*.
8. Paris, P. C., and Erdogan, F., (1963). "A Critical Analysis of Crack Growth Propagation Laws". *Journal of Basic Engineering, 85, pp.528-534*.
9. Bannantine, J. A., Jess, J., Comer, Handrock, J. L., "Fundamentals of Metal Fatigue Analysis". *Prentice Hall, Englewood Cliffs, New Jersey 07632, ISBN 0-13-340191-X*.
10. Mlikota, M., Staib, S., Schmauder, S., and Božić, Ž., "Numerical Determination of Paris Law Constants for Carbon Steel Using a Two-Scale Model". *Materials Research Foundations 114(2022)1-15, https://doi.org/ 10.21741/9781 644 9 01656-1*.
11. Seles, K., Aldakheel, F., Tonkovic, Z., Soric, J., and Wriggers, P., "A General Phase Field Model for Fatigue Failure in Brittle and Ductile Solids". *Computational Mechanics (2021) 67:1431-1452, https:// doi.org /10.1007/s00466-021-01996-5*.

